CVI
Journals.ASM.org

Analysis of Defined Combinations of Monoclonal Antibodies in Anthrax Toxin Neutralization Assays and Their Synergistic Action

Miriam M. Ngundi,[a] Bruce D. Meade,[b] Stephen F. Little,[c] Conrad P. Quinn,[d] Cindi R. Corbett,[e] Rebecca A. Brady,[a] and Drusilla L. Burns[a]

Center for Biologics Evaluation and Research, Food and Drug Administration, Bethesda, Maryland, USA[a]; Meade Biologics, Hillsborough, North Carolina, USA[b]; U.S. Army Medical Research Institute of Infectious Diseases, Fort Detrick, Maryland, USA[c]; National Center for Immunization and Respiratory Diseases, Centers for Disease Control and Prevention, Atlanta, Georgia, USA[d]; and National Microbiology Laboratory, Public Health Agency of Canada, Winnipeg, Manitoba, Canada[e]

Antibodies against the protective antigen (PA) component of anthrax toxin play an important role in protection against disease caused by *Bacillus anthracis*. In this study, we examined defined combinations of PA-specific monoclonal antibodies for their ability to neutralize anthrax toxin in cell culture assays. We observed additive, synergistic, and antagonistic effects of the antibodies depending on the specific antibody combination examined and the specific assay used. Synergistic toxin-neutralizing antibody interactions were examined in more detail. We found that one mechanism that can lead to antibody synergy is the bridging of PA monomers by one antibody, with resultant bivalent binding of the second antibody. These results may aid in optimal design of new vaccines and antibody therapies against anthrax.

Inhalation anthrax, caused by the Gram-positive bacterium *Bacillus anthracis*, is a disease that is associated with high rates of morbidity and mortality if not treated early. The potential use of *B. anthracis* spores as a biological warfare and bioterror agent has spurred significant efforts toward the development of countermeasures for anthrax (16), including new-generation anthrax vaccines and therapeutics. Most anthrax vaccines and therapeutic antibodies that are currently under development are designed to protect against disease by targeting anthrax toxin, a major virulence factor of *B. anthracis* that is believed to play a critical role in disease progression (27, 36).

Anthrax toxin is a tripartite toxin comprising protective antigen (PA), lethal factor (LF), and edema factor (EF). PA combines with LF and EF to form lethal toxin (LT) and edema toxin (ET), respectively (2, 8, 11, 17). Anthrax toxin is believed to be important for outgrowth and trafficking of the bacteria during disease as well as the progression and lethal nature of the disease (2, 10, 12, 19, 25, 27, 36). Because PA is a common component of both ET and LT, most new anthrax vaccines and antibody therapies target PA specifically (9, 14). Anti-PA antibodies have been shown to neutralize anthrax toxin *in vitro* and confer protection in various animal models (13, 20, 21, 31, 41, 42), with levels of neutralizing antibodies correlating with protection (21, 35, 41). For this reason, assessment of toxin neutralization will likely play an important role in the evaluation of new PA-based vaccines and therapeutic antibodies.

Evidence suggests that interplay between antibodies against bacterial toxins can occur as they neutralize their target antigen. In a study of the neutralization of botulinum toxin by monoclonal antibodies (MAbs), Nowakowski and colleagues demonstrated that a combination of MAbs resulted in synergistic neutralization of that toxin. In that study, although no single MAb effectively neutralized the toxin, combinations of three MAbs resulted in significant neutralization both *in vivo* and *in vitro* (30). Those results suggest that a good understanding of the interplay between anti-PA antibodies that might occur as they neutralize their target antigen could provide valuable information for optimal design of antibody therapies and new vaccines against anthrax.

Toxin neutralization by a mixture of antibodies would be expected to be complex in that neutralization depends, at least in part, on the array of epitopes recognized by the antibodies, the binding affinities of the antibodies, the immunoglobulin classes present, and any interactions that may occur between the antibodies and components of the toxin's target cell, e.g., Fcγ receptors (1, 7, 26, 34, 39, 40). While some anthrax toxin-neutralizing antibodies act exclusively by directly interfering with a critical aspect of toxin action, other antibodies neutralize anthrax toxin by a mechanism that includes an Fcγ receptor-mediated component (1, 28, 40). Another class of anti-PA antibody that enhances LT-mediated cytotoxicity through an Fcγ receptor-dependent mechanism has been described previously (24, 28).

Additive, synergistic, or even antagonist interactions between anti-PA antibodies present in a defined mixture of anti-PA monoclonal antibodies or between antibodies induced by vaccination with PA-based vaccines might be expected to occur. In order to better understand the interplay between anti-PA antibodies, PA, and target cell components that may occur, we evaluated toxin neutralization using both individual anti-PA MAbs and combinations of those antibodies. In this study, we examined partially neutralizing, fully neutralizing, and toxicity-enhancing MAbs in cell culture assays using cell types that either do or do not express Fcγ receptors to determine whether the interplay between the antibodies, PA, and the target cell can result in additive, synergistic, and/or antagonistic effects.

Received 9 January 2012 **Returned for modification** 1 February 2012
Accepted 14 March 2012
Published ahead of print 21 March 2012
Address correspondence to Drusilla L. Burns, drusilla.burns@fda.hhs.gov.

doi:10.1128/CVI.05714-11

MATERIALS AND METHODS

Monoclonal antibodies. AVR1046 was prepared in a manner similar to that previously described by Boyer et al. (3). Briefly, 8- to 10-week-old BALB/c mice were immunized subcutaneously with 100 μg of anthrax recombinant PA adjuvanted with Ribi (Ribi ImmunoChem Research, Inc., Hamilton, MT). Booster doses were given on days 21 and 35. On day 38, spleens were harvested and primary splenocytes were isolated. Splenocytes were fused with the mouse myeloma cell line SP 2/0 at a ratio of 1:5 (myeloma/splenocytes) in the presence of polyethylene glycol (PEG) 4000 (Sigma, St. Louis, MO) and treated as described previously (3). Cell culture supernatants were screened for anti-PA antibodies. Anti-PA-producing hybridomas were subcloned three times for isolation of antibody-producing cells. Generated MAbs were further screened for their ability to neutralize LT activity in a J774A.1 cell-based assay (18). F20G75 and 2F9 were prepared and characterized as described by Gubbins et al. (15) and Little et al. (22), respectively. *B. anthracis* protective antigen antibody 18720 (C3), subsequently referred to in this report as C3, was purchased from QED Bioscience, Inc. (San Diego, CA).

Reagents. Anthrax recombinant PA (NR-140 and NR-164), recombinant LF (NR-142), and recombinant EF (NR-2630) and murine macrophage-like J774A.1 cells (NR-28) were from the NIH Biodefense and Emerging Infections Research Resources Repository, National Institute of Allergy and Infectious Diseases (NIAID), NIH (Bethesda, MD). The PA used in this study was verified by sodium dodecyl sulfate-polyacrylamide gel electrophoresis to be >95% full length. Epithelial cell-like CHO-K1 cells were purchased from the American Type Culture Collection (ATCC; Manassas, VA). Rat anti-mouse CD16/CD32 clone 2.4G2 was obtained from BD Pharmingen (Franklin Lakes, NJ).

TNA assays. J774A.1 cells were cultured in Dulbecco's modified Eagle media (DMEM) containing 4.5 g/liter D-glucose and 110 mg/liter sodium pyruvate and supplemented with 5% heat-inactivated bovine serum, 2 mM L-glutamine, penicillin (25 units/ml), streptomycin (25 μg/ml), and 10 mM HEPES. The J774A.1 cell-based toxin-neutralizing antibody (TNA) assay was performed as previously described (29). Briefly, cells were grown for 72 or 96 h in culture flasks at 37°C, 5% CO_2, and 95% relative humidity. The cells were harvested, seeded in 96-well tissue culture plates (40,000 cells/well), and incubated for 17 to 19 h. MAb samples were prepared in a separate 96-well microtiter plate at 2-fold dilutions and stored overnight at 4°C. For assays in which a combination of antibodies was studied, one MAb was serially diluted starting with a concentration approximately equal to its effective concentration at 50% inhibition (EC_{50}) and then the second MAb, at a constant concentration, was spiked into each of the serial dilutions. The spiking concentration was approximately equal to the EC_{50} of the second MAb. The MAb samples were then incubated with a constant concentration of LT (50 ng/ml PA NR-140 and 40 ng/ml LF) for 30 min prior to being added to the cells. The cell-MAb-toxin mix was incubated for 4 h, after which 25 μl per well of 5-mg/ml tetrazolium salt, 3-[4,5-dimethylthiazol-2-yl]-2,5-diphenyltetrazolium bromide (MTT), was added. After a 2-h incubation, the cells were lysed using 100 μl per well of acidified isopropanol (90% isopropanol, 0.5% [wt/vol] SDS, and 38 mM HCl) and the optical density at 570 nm (OD_{570}) was determined, with 690 nm as a reference filter. For assays performed with the Fcγ receptor-blocking MAb 2.4G2, cells were preincubated with 100 μl of 10-μg/ml MAb 2.4G2 for 15 min prior to addition of the MAb-toxin mix. MAb 2.4G2 remained on the cells during the intoxication step.

CHO cells were grown in Kaighn's modified F-12 nutrient mixture containing L-glutamine and supplemented with 10% heat-inactivated bovine serum, 2 mM L-glutamine, penicillin (25 units/ml), and streptomycin (25 μg/ml). The CHO cell-based TNA assay was performed as previously described (29). Briefly, cells and MAb samples were treated as in the J774A.1 cell-based assay, except that the plated cells were incubated for approximately 22 h before addition of the MAb-toxin mix and that ET (50 ng/ml PA NR-140 and 160 ng/ml EF) was used instead of LT. To prevent cyclic AMP (cAMP) degradation, the MAb-toxin mix contained 750 μM 3-isobutyl-1-methylxanthine. After the 4-h incubation, cells were washed three times with medium and cAMP was estimated using the Tropix chemiluminescent cAMP enzyme-linked immunosorbent assay (ELISA) kit (Applied Biosystems, Foster City, CA) in accordance with the manufacturer's instructions. The ELISA output was measured as relative luminescence units (RLU) with 1-s integration. Since this is a competitive assay, the measured RLU values are inversely proportional to the amount of cAMP produced by the cells and therefore higher RLU values reflect greater toxin neutralization.

Competitive ELISA. Ninety-six-well plates (Maxisorp; Nalge Nunc International, Rochester, NY) were coated with 1 μg/ml PA (NR-164) in phosphate-buffered saline (PBS) at 100 μl/well overnight at 4°C. Meanwhile, serial dilutions of PA (NR-164) containing biotinylated MAb AVR1046-IgG (0.13 pmol/ml) or biotinylated AVR1046 Fab fragments (3.4 pmol/ml) in the presence or absence of MAb 2F9 (0.73 pmol/ml) in diluent buffer (1× PBS, pH 7.4, containing 0.5% Tween 20 and 5% nonfat dry milk) were prepared in a separate plate and stored overnight at 4°C. PA-coated plates were washed three times with wash buffer (1× PBS, pH 7.4, containing 0.1% [vol/vol] Tween 20), and 100 μl/well of the PA-antibody samples was transferred to the coated plates and incubated for 1 h at 37°C. The plates were washed three times with wash buffer, and 100 μl per well of goat anti-biotin-IgG conjugated to horseradish peroxidase (HRP) (Cell Signaling Technology, Danvers, MA) was added. The plate was incubated for 1 h at 37°C and washed three times, and 100 μl per well of 2,2-azinobis(3-ethylbenzthiazolinesulfonic acid) (ABTS) (KPL, Gaithersburg, MD) was added for color development. After a 30-min incubation at 37°C, 100 μl per well of ABTS peroxidase stop solution (KPL, Gaithersburg, MD) was added and the OD was read at 405 nm, with 490 nm as a reference filter.

Mapping of MAb binding to PA. The individual protein domains of PA, which are composed of amino acids 1 to 258 (domain 1), 259 to 487 (domain 2), 488 to 595 (domain 3), and 596 to 735 (domain 4) were cloned into *Escherichia coli* strain BL21, expressed, and purified as described previously (4). Each recombinant domain was resolved by SDS-PAGE and transferred to nitrocellulose for immunoblotting. The blots were blocked with 5% nonfat dry milk in 10 mM Tris-buffered saline (TBS), pH 7.3, containing 0.1% (vol/vol) Tween 20 and then probed with each monoclonal antibody at an appropriate dilution. Sheep anti-mouse IgG–HRP (GE Healthcare, Piscataway, NJ) was utilized as a secondary antibody, and reactivity was visualized using a chemiluminescent substrate (Amersham ECL; GE Healthcare).

Fab fragment preparation and biotinylation of IgGs and Fab fragments. AVR1046-Fab fragments were prepared from AVR1046-IgG using a mouse IgG1 Fab and $F(ab')_2$ preparation kit (Pierce, Rockford, IL) according to the manufacturer's instructions. Additional purification was performed using fast protein liquid chromatography (FPLC) with a Superdex 200, 10/300 GL column (GE Healthcare Biosciences, Pittsburgh, PA). Purified Fab fragments were concentrated and stored in 1× PBS at 4°C.

AVR1046-IgG and AVR1046-Fab fragments were biotinylated using EZ-Link NHS-LC-biotin [succinimidyl-6-(biotinamido)hexanoate; Pierce, Rockford, IL]. The IgG and Fab samples were incubated with 5-fold molar excess biotin in 50 mM bicarbonate buffer, pH 8.5, for 30 min. Labeled IgG was separated from unincorporated biotin by size exclusion chromatography using a BioGel P10 column (Bio-Rad, Hercules, CA) with UV-visible (UV-Vis) detection at 280 nm. Labeled Fab fragments were purified using a desalting column (Pierce, Rockford, IL). Biotinylated IgG and Fab fragments were concentrated to approximately 1 mg/ml and stored in 1× PBS at 4°C. The concentrations of the biotinylated IgG and Fab fragments were determined using UV-Vis absorbance at 280 nm, with extinction coefficients of 1.43 and 1.53, respectively.

Data and statistical analyses. For TNA assays, OD_{570} and RLU values for the cell-only control, run on the same plate as the sample, were set to 100%. Percent viability and RLU for samples were then calculated relative to the OD_{570} and RLU, respectively, for the cell-only control. All data were plotted using PRISM 5 software (GraphPad Software Inc., La Jolla, CA).

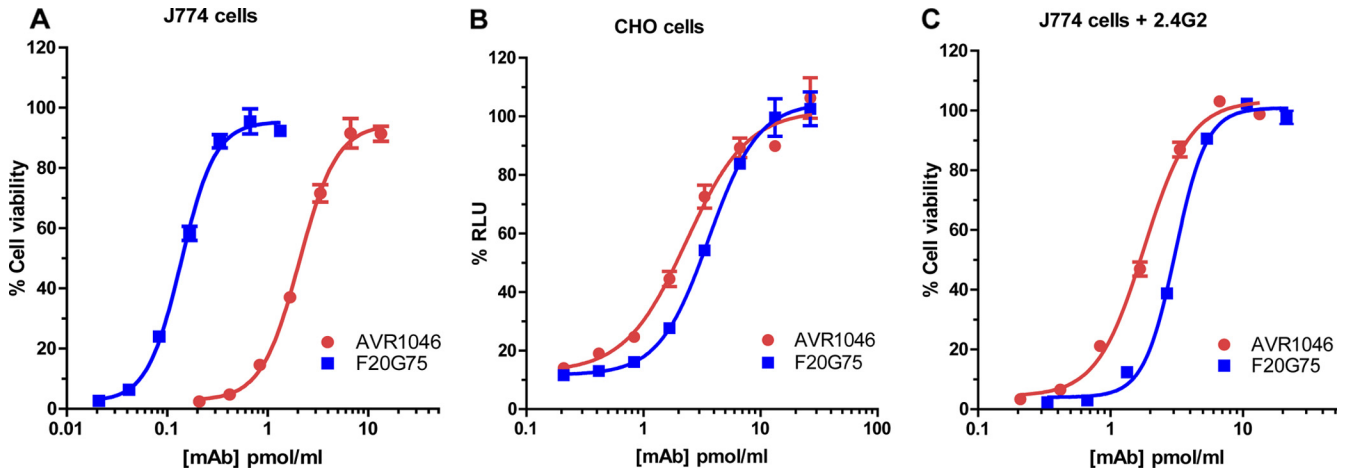

FIG 1 Concentration dependence curves for the neutralization of protective antigen by MAbs AVR1046 and F20G75 in the J774A.1 and CHO cell-based assays. The indicated concentrations of MAb AVR1046 and MAb F20G75 were used to neutralize a constant concentration of either LT in the J774A.1 cell-based assay (A and C) or ET in the CHO cell-based assay (B). In panel C, FcγRIIB/III receptors were blocked by the addition of MAb 2.4G2 as described in Materials and Methods. Each point corresponds to the mean of the values obtained for three independent sample preparations, with the standard deviation (SD) indicated by the error bar. The samples were run on duplicate plates for the J774.1A cell-based assay and on a single plate for the CHO cell-based assay. Each curve is representative of three independent assays run on different days.

The neutralizing activities of MAbs were calculated using curve fitting analyses performed in GraphPad PRISM 5 software. Specifically, a four-parameter logistic (4-PL) regression model was used to fit the percent viability or percent RLU versus the concentration of the antibody. Reported EC_{50} is the inflection point for each curve from this model that represents 50% inhibition for the corresponding antibody. For data that did not exhibit a symmetrical sigmoidal shape, bell-shaped dose-response curves were used to draw a smooth curve through the data. For data interpretation and discussion, synergistic neutralization was reported when neutralization activity of a combination of two MAbs was greater than the sum of neutralization activities of the individual MAbs at any given concentration. Similarly, additive neutralization was reported when the neutralization activity yielded by a combination of two MAbs approximated the sum of the MAbs' individual neutralization activities at a given concentration. For competitive ELISA, OD_{405} readings for each curve were normalized to the OD_{405} of its upper asymptote, set as 100%, and the curves were then fitted using a nonlinear 4-PL curve fit model.

RESULTS

Analysis of selected individual MAbs in TNA assays. Two TNA assay formats have been widely used in both research and clinical studies to assess the ability of anti-PA antibodies to neutralize anthrax toxin (1, 6, 15, 22–24, 28, 37, 40). The two formats are the J774A.1 cell-based TNA assay and the Chinese hamster ovary (CHO) cell-based TNA assay. These assays differ both in the cell substrate and in the particular toxin—LT or ET—used to assess neutralization of PA action. J774A.1 cells are murine macrophage-like cells that express Fcγ receptors (33, 39). The TNA assay based on these cells measures neutralization of the cytocidal activity of LT. CHO cells are epithelial cells that do not express Fcγ receptors (32). The TNA assay that utilizes CHO cells measures the ability of antibodies to neutralize ET-induced increases in intracellular cAMP levels.

For this study, we screened 25 MAbs for toxin neutralization in both assays. We identified three categories of MAbs based on their neutralization behaviors. The first category was MAbs which were nonneutralizing in both assays, the second was MAbs which neutralize toxin in both assays, and the third was MAbs which were nonneutralizing in the J774A.1 cell assay but neutralizing in the CHO cell assay. For further studies, we chose two MAbs from each of the second and third categories.

Figure 1 shows the neutralization curves in the two assays for two neutralizing MAbs, AVR1046 and F20G75. AVR1046 is a murine IgG1 (18). We mapped the epitope for this MAb to domain 4 (amino acids 596 to 735) of PA, the receptor binding domain, using purified PA domains and immunoblot analysis as described in Materials and Methods (data not shown). F20G75 is also a murine IgG1; this MAb binds to a loop region extending from amino acid 304 to 319, found in domain 2 of PA, which is believed to be involved in pore formation (15). In the J774A.1 cell-based assay (Fig. 1A), EC_{50}s for F20G75 and AVR1406 were 0.1 pmol/ml and 1.7 pmol/ml, respectively (geometric means of three independent assays), indicating that F20G75 was significantly more neutralizing than AVR1046 on a molar basis ($P = 0.0004$; unpaired t test) in that assay. In the CHO cell-based assay (Fig. 1B), the EC_{50}s were 1.7 pmol/ml and 2.7 pmol/ml for AVR1046 and F20G75, respectively (geometric means of three independent assays). A comparison of the neutralization of AVR1046 to that of F20G75 in the J774A.1 cell-based assay showed that F20G75 was 17 times more effective than AVR1046 on a molar basis, but in the CHO cell assay, no significant difference in neutralization was observed ($P = 0.15$; unpaired t test). In order to determine whether Fcγ receptors, which are present on J774A.1 cells but absent on CHO cells, may have played a role in the striking difference in relative neutralization between the two antibodies in the two different assays, we blocked the major Fcγ receptors (IIB and III) expressed by J774A.1 cells using the Fcγ receptor-blocking MAb 2.4G2 (38). As shown in Fig. 1C, when these Fcγ receptors were blocked, the EC_{50} for AVR1046 was 1.7 pmol/ml (geometric mean of three independent assays), which was identical to the value observed without blocking the same receptors, indicating that AVR1046 neutralization has no Fcγ receptor-mediated component. In contrast, the EC_{50} for F20G75 was 3.1 pmol/ml (geometric mean of two independent assays), which was significantly different from

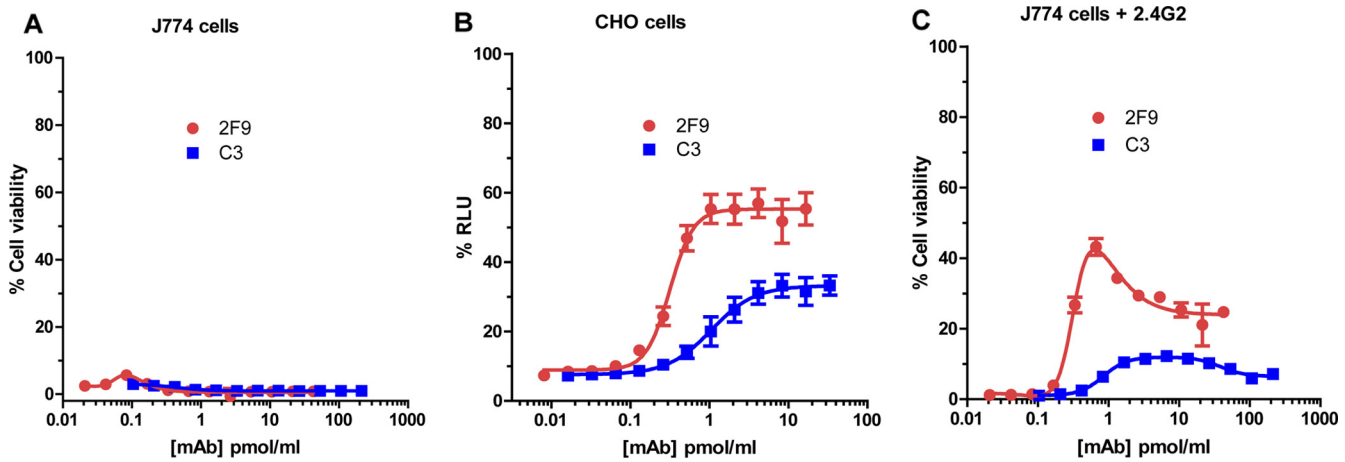

FIG 2 Concentration dependence curves for the neutralization of protective antigen by MAbs 2F9 and C3 in the J774A.1 and CHO cell-based assays. The indicated concentrations of MAb 2F9 and MAb C3 were used to neutralize a constant concentration of either LT in the J774A.1 cell-based assay (A and C) or ET in the CHO cell-based assay (B). In panel C, FcγRIIB/III receptors were blocked by the addition of MAb 2.4G2 as described in Materials and Methods. Each point corresponds to the mean of the values obtained for three independent sample preparations, with the SD indicated by the error bar. The samples were run on duplicate plates for the J774.1A cell-based assay and on a single plate for the CHO cell-based assay. Each curve is representative of three independent assays each run on different days.

the value obtained for the same MAb when the Fcγ receptors were not blocked ($P < 0.0001$; unpaired *t* test). This result indicates that Fcγ receptors play a major role in the neutralization of toxin by F20G75 in the J774A.1 cell-based assay.

Figure 2 shows the neutralization curve for two MAbs, 2F9 and C3, belonging to the category of MAbs that are nonneutralizing in our J774A.1 cell assay but partially neutralizing in the CHO cell assay. 2F9 is a murine IgG1 antibody (22), as is C3 (manufacturer's literature). We have mapped the binding of 2F9 to domain 3 (amino acids 488 to 595) of PA, which is involved in heptamerization, and the binding of C3 to domain 4 of PA (amino acids 596 to 735) (data not shown). These MAbs (2F9 and C3) exhibited nonneutralizing behavior in the J774A.1 cell-based assay using our routine assay conditions, which include fully cytotoxic concentrations of LT (Fig. 2A). Of note, others have previously shown that, when 2F9 is used in a modified form of the J774 assay in which sublethal concentrations of LT are used, 2F9 increases cytotoxicity (24, 28). However, in our assay, since we are using fully lethal concentrations of LT, we would not expect to be able to observe such an enhancement of cytoxicity. When we examined 2F9 and C3 in the CHO cell-based assay, both MAbs exhibited some neutralizing activity (Fig. 2B), with EC_{50}s of 0.2 pmol/ml and 0.8 pmol/ml, respectively (geometric means of four independent assays). Of note, however, neither MAb exhibited complete protection regardless of the amount of MAb used, as manifested by an upper asymptote of the neutralization curve of less than 100% RLU. The neutralizing capacity of C3 reached a plateau at a lower RLU value than that for 2F9. While 2F9 and C3 did not exhibit measurable neutralization in the J774A.1-based assay, blocking Fcγ receptors of the cells renders the MAbs partially neutralizing (Fig. 2C). The neutralization curves are not typical concentration dependence curves; rather, cell viability initially increased with increasing antibody concentration and then decreased at higher antibody concentrations. While we do not know the reason for the biphasic nature of the neutralization curves, one possibility is that Fcγ receptors I and IV may play a role in the decrease in neutralization seen at the higher MAb levels, since these Fcγ receptor types are not blocked by the Fcγ receptor blocking MAb 2.4G2 (38). Perhaps only at higher concentrations of 2F9 and C3 do sufficient interactions between the MAbs and Fcγ receptors I and IV occur to lead to Fcγ receptor-dependent enhanced toxicity involving these receptor types, resulting in the observed drop in neutralization.

Analysis of combinations of MAbs in TNA assays. The production of different types of MAbs (neutralizing, nonneutralizing, and cytotoxicity enhancing) against PA suggests the likely presence of these diverse antibodies in any given polyclonal antibody preparation. Here we investigate the resultant neutralization exhibited by pairwise combinations of MAbs. In order not to saturate neutralization, one MAb was serially diluted starting at a concentration approximately equal to its EC_{50}. The second MAb was then added at a constant concentration, also approximately equal to its EC_{50}, to the serial dilutions of the first MAb. For comparison purposes, serial dilutions of the first MAb alone were also assayed.

Figure 3 shows the neutralization of toxin by a combination of AVR1046 with F20G75 (both neutralizing individually). When a mixture of F20G75 at its EC_{50} (0.13 pmol/ml) and increasing concentrations of AVR1046 was used to neutralize LT in the J774A.1 cell-based assay, a decrease in cell viability was initially observed. As more AVR1046 was added, the initial decrease was followed by an increase in cell viability (Fig. 3A). The minimum cell viability (dip) was observed at an AVR1046 concentration of 0.13 pmol/ml, a concentration equivalent to that of added F20G75. Toxin neutralization by either AVR1046 or F20G75 alone did not exhibit such a decrease in cell viability. A partially additive effect of the MAbs was observed at the higher concentrations of AVR1046. When Fcγ receptors IIB and III were blocked, synergistic neutralization was observed with the antibody combination compared to the individual antibodies (Fig. 3B), with no indication of the antagonistic effect that had been observed when Fcγ receptors were not blocked. Please note, however, that because the EC_{50} of F20G75 is greater when Fcγ receptors are blocked (3.1 pmol/ml) (Fig. 1), F20G75 was used at a 10-fold-higher concentration in this

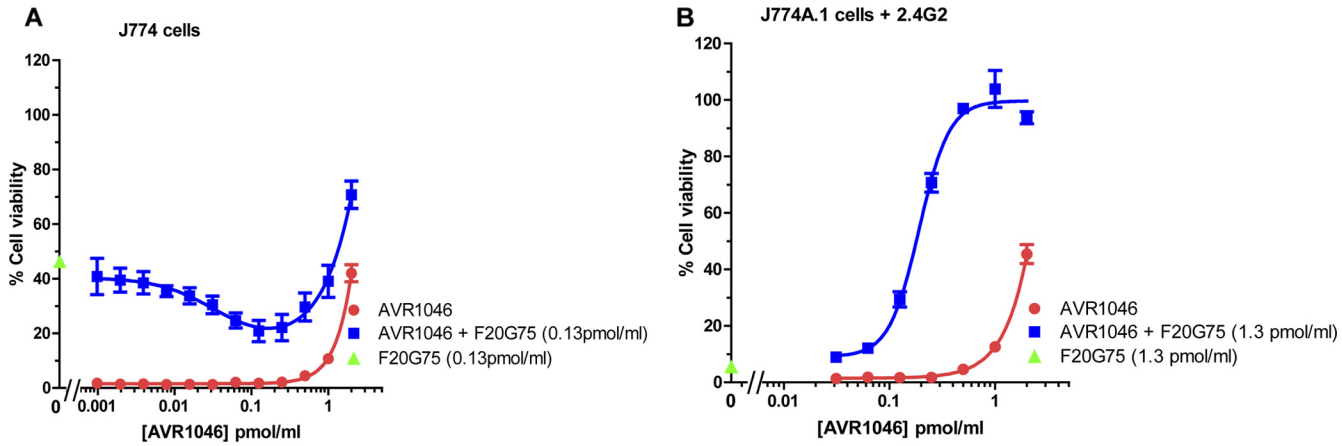

FIG 3 Concentration dependence curves for toxin neutralization by the combination of MAbs AVR1046 and F20G75. The concentration of one antibody was varied in the manner indicated on the *x* axis, while that of the other was held constant. Cell viability is indicated for concentrations of the serially diluted antibody assayed either individually or combined with the other MAb held constant at the concentration indicated. Neutralization obtained with the antibody that was held constant in the absence of the serially diluted antibody is indicated on the *y* axis. In panel B, assays were conducted in the presence of the Fcγ receptor-blocking antibody MAb 2.4G2 as described in Materials and Methods. Each point corresponds to the mean of the values obtained for three independent sample preparations run on the same plate, with the SD indicated by the error bar. For each independent assay, the samples were run on duplicate plates. Each curve is representative of independent assays each run on at least three different days.

experiment than in the experiment utilizing unblocked cells (0.1 pmol/ml) (Fig. 3A).

Studies of the combination of MAb AVR1046 with MAb 2F9 were also conducted. Synergistic toxin neutralization was observed in the J774A.1 cell assay for serial dilutions of AVR1046 with a constant concentration of 2F9 (Fig. 4A) or serial dilutions of 2F9 with a constant concentration of AVR1046 (Fig. 4B). Finally, we examined the combination of MAbs 2F9 and C3. As described above, when assayed individually in our J774A.1 cell-based assay, neither MAb exhibited neutralizing activity (Fig. 2A); however, in the CHO cell-based assay, they were both partially neutralizing (Fig. 2B). Surprisingly, the MAb combination showed a robust synergistic neutralization of LT in the J774A.1 cell-based assay (Fig. 5A and B). Synergy was observed regardless of which MAb was serially diluted. In the CHO cell-based assay, when the two MAbs were combined, neutralization appeared to be additive (Fig. 5C and D) regardless of which MAb was serially diluted.

Investigation of the mechanism underlying synergistic neutralization. Nowakowski et al. (30) demonstrated that synergistic neutralization of botulinum toxin by multiple antibodies was a result of an increase in functional binding affinity. Those investigators suggested that an increase in functional binding affinity could be due to the binding of one IgG antibody to two toxin molecules, which could then favor bivalent binding of the second antibody with a resultant increase in antibody avidity, with avidity being the combined strength of multiple bond interactions. Alternatively, the binding of the first antibody might induce or stabilize

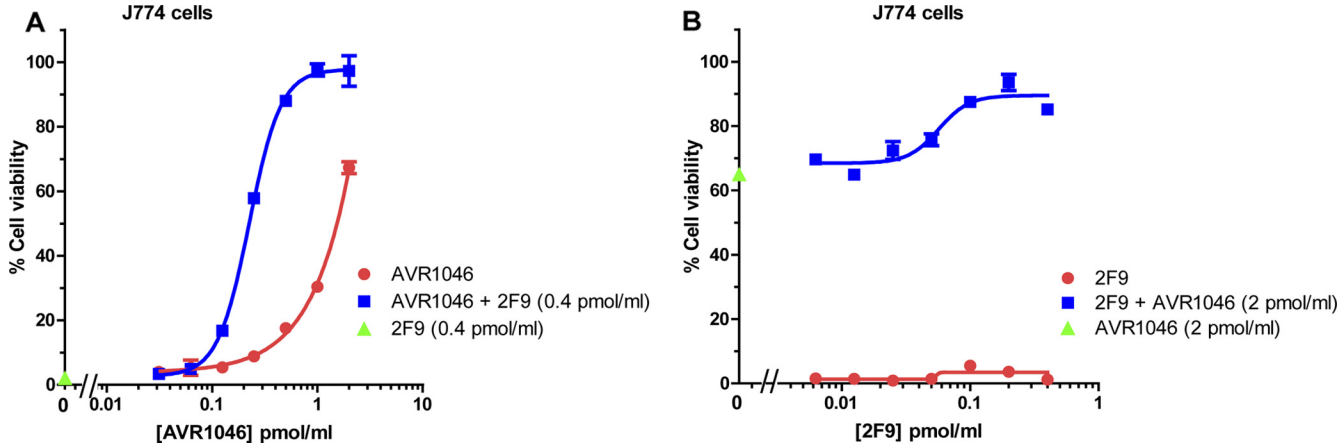

FIG 4 Concentration dependence curves for toxin neutralization of protective antigen by the combination of MAbs AVR1046 and 2F9. The concentration of one antibody was varied in the manner indicated on the *x* axis, while that of the other was held constant. Cell viability is indicated for concentrations of the serially diluted antibody assayed either individually or combined with the other MAb held constant at the concentration indicated. Neutralization obtained with the antibody that was held constant, in the absence of the serially diluted antibody, is indicated on the *y* axis. Each point corresponds to the mean of the values obtained for three independent sample preparations, with the SD indicated by the error bar. For each independent assay, samples were run on duplicate plates. Each curve is representative of three independent assays each run on different days.

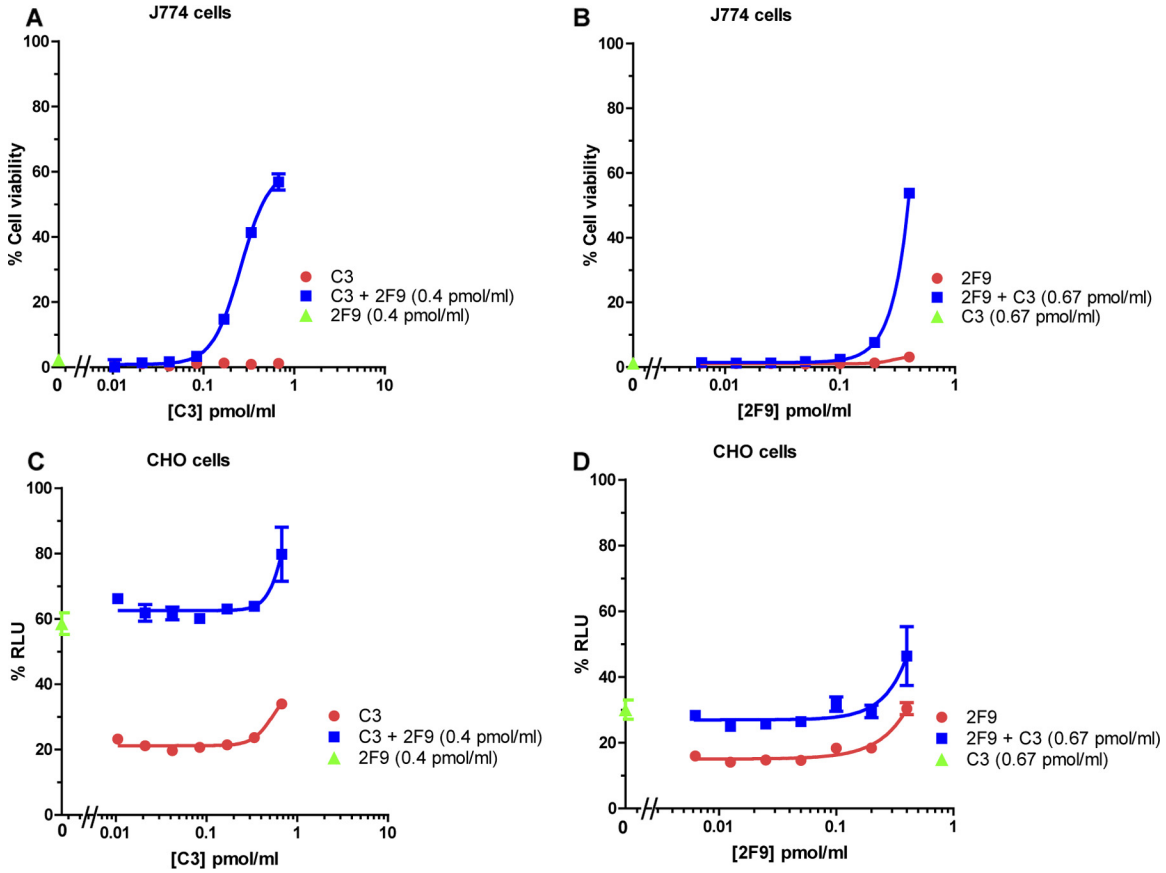

FIG 5 Concentration dependence curves for toxin neutralization by the combination of MAbs C3 and 2F9. The concentration of one antibody was varied in the manner indicated on the *x* axis, while that of the other was held constant. Cell viability in the J774A.1 cell-based assay (A and B) or % RLU in the CHO cell-based assay (C and D) is indicated for concentrations of the serially diluted antibody assayed either individually or combined with the other MAb held constant at the concentration indicated. Neutralization obtained with the antibody that was held constant, in the absence of the serially diluted antibody, is indicated on the *y* axis. Each point corresponds to the mean of the values obtained for three independent sample preparations, with the SD indicated by the error bar. For each independent assay, samples were run on duplicate plates. Each curve is representative of three independent assays each run on different days.

a conformation of the toxin that favors the binding of the second antibody. Those investigators did not further investigate which of these mechanisms might underlie the increase in functional binding that they observed.

We reasoned that similar mechanisms might be the basis for the synergy between the PA MAbs that we observed. To investigate whether binding of 2F9 to PA could "convert" PA to a multivalent antigen by bridging PA monomers—thereby facilitating bivalent binding of AVR1046—we utilized AVR1046 Fab fragments in a competitive ELISA and compared the results to those obtained using AVR1046 IgG. While IgG can bind bivalently, Fab fragments are limited to monovalent binding. By comparing the binding properties of the AVR1046 IgG and its Fab fragments, we would be able to evaluate whether 2F9 induces bivalent binding of AVR1046 to PA molecules.

Because we believe that soluble PA better represents the biologically relevant form of PA, for these experiments we used a competitive ELISA format, instead of the normal indirect ELISA, in order to measure binding to PA in solution rather than to PA bound to the plastic plate. In this competitive ELISA, serial dilutions of PA were incubated with constant amounts of antibodies or Fab fragments overnight at 4°C to allow binding to reach equilibrium. The PA-antibody mixtures were then added to 96-well plates that had been coated with PA. In order to assess AVR1046 binding in a manner that distinguishes it from that of 2F9, the AVR1046 IgG and Fab fragments used in the assay were biotinylated and detected in the assay using an antibiotin-HRP conjugate. In this competition assay, one would expect that, as the concentration of soluble PA is increased, more of the AVR1046 would become bound to this species and therefore less would be available for binding to the PA-coated plate. The concentration of soluble PA that is required for 50% inhibition of AVR1046 binding to the PA coating the plate (IC_{50}) can be measured. If 2F9 increases the avidity of AVR1046 or AVR1046 Fab fragments for the soluble PA, then the amount of soluble PA needed to prevent the binding of AVR1046 or AVR1046 Fab fragments to the PA-coated plate should decrease (i.e., the IC_{50} for soluble PA would decrease).

Figure 6A shows that the concentration of soluble PA needed to prevent binding of biotinylated AVR1046 IgG to the PA-coated plate was significantly less in the presence of 2F9 than in its absence (i.e., the observed IC_{50} decreases in the presence of 2F9, reflective of an increase in the avidity of AVR1046 for soluble PA). In contrast (Fig. 6B), the amounts of soluble PA needed to prevent binding of biotinylated AVR1046 Fab fragments to the PA-coated plate were similar in the presence or absence of 2F9 (i.e., no change in IC_{50} for soluble PA, reflective of no change in the avidity of

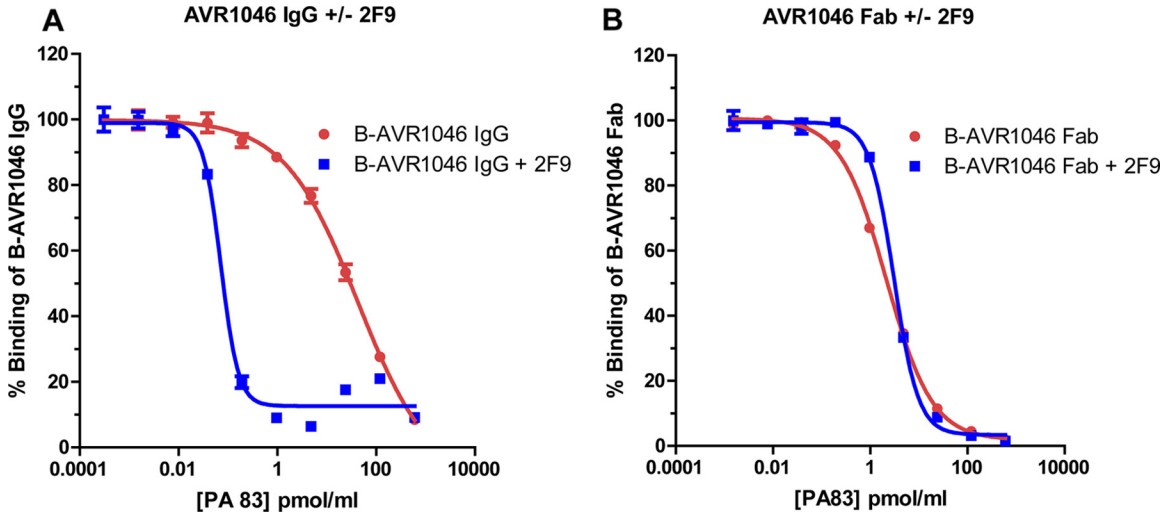

FIG 6 Analysis of MAb AVR1046 binding in the presence or absence of MAb 2F9 using a competitive PA ELISA with soluble PA as the competitor. The indicated concentrations of soluble PA mixed with either biotinylated AVR1046 IgG (B-AVR1046) in the absence and presence of 2F9 (A) or B-AVR1046 Fab fragments in the absence and in the presence of 2F9 (B) were assayed for binding using the competitive ELISA format described in Materials and Methods. The ability of soluble PA to inhibit binding of B-AVR1046 or B-AVR1046 Fab fragments to the PA coating the plate was determined. The OD_{405} readings for each competition curve were normalized to the OD_{405} of its upper asymptote, set as 100%, and the data points were then fitted using a 4-PL regression model. Each point corresponds to the mean of the values obtained for three independent sample preparations run on the same plate, with the SD indicated by the error bar. Each figure is representative of the three independent assays, each run on different days.

AVR1046 Fab fragments for PA). Thus, 2F9 increased the avidity of a form of AVR1046 that has two binding sites for PA but not of a form that has only a single PA binding site. This observation suggests that 2F9 can promote bivalent binding of AVR1046 IgG to PA, presumably by bridging two PA monomers.

DISCUSSION

In the course of this study, two major findings emerged. First, assessment of the neutralizing capacity of any particular antibody can be highly dependent on the TNA assay used. Second, the interplay between antibodies, PA, and any Fcγ receptors that may be present can result in additive, synergistic, or antagonistic interactions.

The first important aspect of this work is our finding that different TNA assays can give strikingly different impressions of antibody neutralization. As seen in Fig. 1, MAb F20G75 was significantly more neutralizing than AVR1046 in the J774A.1 cell-based assay, but the two antibodies exhibited approximately the same neutralizing capacity in the CHO cell-based assay. We found that this difference was likely due, at least in part, to the fact that neutralization by F20G75 is highly dependent on Fcγ receptors (Fig. 1C). Because of this Fcγ receptor dependence, very different impressions of the neutralizing capacity of this MAb are given by the two different assays. These results raise the question of which assay more accurately reflects antibody neutralization of anthrax toxin *in vivo*. Pertinent to this question are the recent findings of Abboud et al., who reported that passive immunization with an anti-PA MAb protected wild-type mice, but not FcγR-deficient mice, against *B. anthracis* infection (1), suggesting that Fcγ receptors do play a role in toxin neutralization or toxin clearance *in vivo*. While more work is needed to make definitive conclusions concerning which assay is more relevant to antibody neutralization *in vivo*, our work suggests that careful thought should be given the choice of the assay when assigning and/or comparing the neutralization activities of MAbs.

A second aspect of our study demonstrates that the interplay between antibodies, PA, and any Fcγ receptors that may be present on target cells can result in several different types of interactions. Additive interactions between antibodies, which have been reported previously for antibody binding to PA (5), were found and would be expected since PA is sufficiently large to bind to more than one antibody at a time. While others have previously reported that one antibody directed to PA combined with another directed to LF provided synergistic protection *in vivo* (6), to our knowledge, synergism between two PA antibodies has not been demonstrated previously. In our study, we found several instances of synergy.

The combination of AVR1046 and 2F9 exhibited synergistic neutralization in the J774A.1 cell assay (Fig. 4). When we examined the molecular basis for the synergy between these antibodies, we found that the binding of 2F9 promoted bivalent binding of AVR1046 (Fig. 6). Because full-length PA is normally found in the monomeric form in solution, these results would suggest that each of these MAbs is capable of bridging PA monomers. Bridging by one of the antibodies would promote bridging by the other. Any transient dissociation of one antibody arm from the antigen would result in rapid rebinding since the other antibody bridge would prevent the antigen from diffusing away. This phenomenon would substantially increase antibody avidity, resulting in synergistic neutralization.

We also observed synergistic neutralization with the combination of AVR1046 and F20G75 in the J774A.1 cell assay (Fig. 3), but only when the majority of Fcγ receptors were blocked (i.e., in the presence of the Fcγ receptor-blocking antibody MAb 2.4G2). The neutralization pattern for this combination of antibodies in the presence of Fcγ receptors was complex and will be discussed

below. Because AVR1046 can bridge two PA monomers, the mechanism underlying the synergy observed may be the same as that discussed above for AVR1046 and 2F9, i.e., induction of bivalent binding.

The combination of MAbs 2F9 and C3 yielded what was perhaps the most surprising result. While neither antibody exhibited any neutralization in our J774A.1 cell-based assay, when the MAbs were mixed together, significant neutralization was observed (Fig. 5A and B). In contrast, this synergy was not observed in the CHO cell-based assay (Fig. 5C and D). The interactions between the two antibodies, PA, and possibly Fcγ receptors that result in synergistic neutralization on J774A.1 cells remain to be elucidated.

In our studies, we noted one instance of antagonistic interactions between antibodies. When the combination of AVR1046 and F20G75 was examined in the J774A.1 cell-based assay (Fig. 3A), a complex pattern, which was highly dependent on Fcγ receptors, was noted. We observed that as the concentration of AVR1046 was increased, an initial antagonism between AVR1046 and F20G75 was observed, as manifested by a decrease in neutralization. As AVR1046 concentration was further increased, neutralization gradually increased. Because neutralization by F20G75 is highly dependent on Fcγ receptors, the initial dip in neutralization that was observed could be explained if AVR1046 prevents the PA-F20G75 complex from binding to Fcγ receptors. Such inhibition might be due to direct steric inhibition of the formation of an F20G75-PA-Fcγ receptor complex by AVR1046. Alternatively, since AVR1046 binds to the receptor binding domain of PA, this antibody may inhibit PA binding to its cell surface receptor, thereby decreasing the effective concentration of PA at the cell surface. This effective decrease in concentration would result in fewer opportunities for a PA-F20G75-Fcγ receptor complex to form. As the concentration of AVR1046 is further increased, neutralization by AVR1046 would be expected to become dominant, consistent with the recovery in neutralization that was observed.

From the results of our study, we can conclude that additive, synergistic, or antagonistic interactions can occur among anti-PA antibodies, PA, and Fcγ receptors that may be present on the cell surface. We have demonstrated that one mechanism that can lead to antibody synergy is the bridging of PA monomers in solution by one antibody, with resultant bivalent binding of the second antibody. Our demonstration of anti-PA antibody synergy suggests that the design of new anthrax antibody therapies and vaccines might be better optimized if these findings are taken into account. For example, appropriate combinations of MAbs, rather than individual antibodies alone, might result in more-favorable therapeutic outcomes. Specifically tailoring new vaccines to modulate the polyclonal response in such a way as to promote synergistic neutralization, while admittedly challenging, might be set as a future goal. In this study, we examined the interplay between anti-PA antibodies exclusively; however, we believe that our findings may apply broadly to neutralizing antibodies against many bacterial toxins.

ACKNOWLEDGMENTS

This work was supported in part by an interagency agreement between the National Institute of Allergy and Infectious Diseases, NIH, and the Food and Drug Administration.

The following reagents were obtained from the NIH Biodefense and Emerging Infections Research Resources Repository, NIAID, NIH: anthrax LF, recombinant from *Bacillus anthracis*, NR-142; anthrax PA, recombinant from *Bacillus anthracis*, NR-140; anthrax PA, recombinant from *Bacillus anthracis*, NR-164; anthrax EF, recombinant from *Bacillus anthracis*, NR-2630; and J774A.1 monocyte/macrophage (mouse) Working Cell Bank, NR-28.

REFERENCES

1. **Abboud N, et al.** 2010. A requirement for FcgammaR in antibody-mediated bacterial toxin neutralization. J. Exp. Med. **207**:2395–2405.
2. **Baldari CT, Tonello F, Paccani SR, Montecucco C.** 2006. Anthrax toxins: a paradigm of bacterial immune suppression. Trends Immunol. **27**:434–440.
3. **Boyer AE, et al.** 2007. Detection and quantification of anthrax lethal factor in serum by mass spectrometry. Anal. Chem. **79**:8463–8470.
4. **Brady RA, Verma A, Meade BD, Burns DL.** 2010. Analysis of antibody responses to protective antigen-based anthrax vaccines through use of competitive assays. Clin. Vaccine Immunol. **17**:1390–1397.
5. **Brossier F, Levy M, Landier A, Lafaye P, Mock M.** 2004. Functional analysis of *Bacillus anthracis* protective antigen by using neutralizing monoclonal antibodies. Infect. Immun. **72**:6313–6317.
6. **Chen Z, et al.** 2009. Novel chimpanzee/human monoclonal antibodies that neutralize anthrax lethal factor, and evidence for possible synergy with anti-protective antigen antibody. Infect. Immun. **77**:3902–3908.
7. **Clement KH, et al.** 2010. Vaccination of rhesus macaques with the anthrax vaccine adsorbed vaccine produces a serum antibody response that effectively neutralizes receptor-bound protective antigen in vitro. Clin. Vaccine Immunol. **17**:1753–1762.
8. **Collier RJ, Young JA.** 2003. Anthrax toxin. Annu. Rev. Cell Dev. Biol. **19**:45–70.
9. **Cybulski RJ, Jr., Sanz P, O'Brien AD.** 2009. Anthrax vaccination strategies. Mol. Aspects Med. **30**:490–502.
10. **Dang O, Navarro L, Anderson K, David M.** 2004. Cutting edge: anthrax lethal toxin inhibits activation of IFN-regulatory factor 3 by lipopolysaccharide. J. Immunol. **172**:747–751.
11. **Duesbery NS, et al.** 1998. Proteolytic inactivation of MAP-kinase-kinase by anthrax lethal factor. Science **280**:734–737.
12. **Ebrahimi CM, Sheen TR, Renken CW, Gottlieb RA, Doran KS.** 2011. Contribution of lethal toxin and edema toxin to the pathogenesis of anthrax meningitis. Infect. Immun. **79**:2510–2518.
13. **Fellows PF, et al.** 2001. Efficacy of a human anthrax vaccine in guinea pigs, rabbits, and rhesus macaques against challenge by Bacillus anthracis isolates of diverse geographical origin. Vaccine **19**:3241–3247.
14. **Friedlander AM, Little SF.** 2009. Advances in the development of next-generation anthrax vaccines. Vaccine **27**:D28–D32.
15. **Gubbins MJ, et al.** 2006. Production and characterization of neutralizing monoclonal antibodies that recognize an epitope in domain 2 of Bacillus anthracis protective antigen. FEMS Immunol. Med. Microbiol. **47**:436–443.
16. **Inglesby TV, et al.** 1999. Anthrax as a biological weapon. JAMA **281**: 1735–1745.
17. **Leppla SH.** 1982. Anthrax toxin edema factor: a bacterial adenylate cyclase that increases cyclic AMP concentrations in eukaryotic cells. Proc. Natl. Acad. Sci. U. S. A. **79**:3162–3166.
18. **Li H, et al.** 2008. Standardized, mathematical model-based and validated *in vitro* analysis of anthrax lethal toxin neutralization. J. Immunol. Methods **333**:89–106.
19. **Li Y, Sherer K, Cui X, Eichacker PQ.** 2007. New insights into the pathogenesis and treatment of anthrax toxin-induced shock. Expert Opin. Biol. Ther. **7**:843–854.
20. **Little SF, Ivins BE, Fellows PF, Friedlander AM.** 1997. Passive protection by polyclonal antibodies against *Bacillus anthracis* infection in guinea pigs. Infect. Immun. **65**:5171–5175.
21. **Little SF, et al.** 2004. Defining a serological correlate of protection in rabbits for a recombinant anthrax vaccine. Vaccine **22**:422–430.
22. **Little SF, Leppla SH, Cora E.** 1988. Production and characterization of monoclonal antibodies to the protective antigen component of *Bacillus anthracis* toxin. Infect. Immun. **56**:1807–1813.
23. **Little SF, et al.** 1996. Characterization of lethal factor binding and cell receptor binding domains of protective antigen of Bacillus anthracis using monoclonal antibodies. Microbiology **142**(Pt. 3):707–715.
24. **Little SF, Webster WM, Fisher DE.** 2011. Monoclonal antibodies directed against protective antigen of Bacillus anthracis enhance lethal toxin activity in vivo. FEMS Immunol. Med. Microbiol. **62**:11–22.

25. **Loving CL, et al.** 2009. Role of anthrax toxins in dissemination, disease progression, and induction of protective adaptive immunity in the mouse aerosol challenge model. Infect. Immun. **77**:255–265.
26. **Maynard JA, et al.** 2002. Protection against anthrax toxin by recombinant antibody fragments correlates with antigen affinity. Nat. Biotechnol. **20**: 597–601.
27. **Moayeri M, Leppla SH.** 2004. The roles of anthrax toxin in pathogenesis. Curr. Opin. Microbiol. **7**:19–24.
28. **Mohamed N, et al.** 2004. Enhancement of anthrax lethal toxin cytotoxicity: a subset of monoclonal antibodies against protective antigen increases lethal toxin-mediated killing of murine macrophages. Infect. Immun. **72**:3276–3283.
29. **Ngundi MM, Meade BD, Lin TL, Tang WJ, Burns DL.** 2010. Comparison of three anthrax toxin neutralization assays. Clin. Vaccine Immunol. **17**:895–903.
30. **Nowakowski A, et al.** 2002. Potent neutralization of botulinum neurotoxin by recombinant oligoclonal antibody. Proc. Natl. Acad. Sci. U. S. A. **99**:11346–11350.
31. **Pitt ML, et al.** 2001. In vitro correlate of immunity in a rabbit model of inhalational anthrax. Vaccine **19**:4768–4773.
32. **Quilliam AL, Osman N, McKenzie IF, Hogarth PM.** 1993. Biochemical characterization of murine Fc gamma RI. Immunology **78**:358–363.
33. **Ravetch JV, et al.** 1986. Structural heterogeneity and functional domains of murine immunoglobulin G Fc receptors. Science **234**:718–725.
34. **Reason D, Liberato J, Sun J, Keitel W, Zhou J.** 2009. Frequency and domain specificity of toxin-neutralizing paratopes in the human antibody response to anthrax vaccine adsorbed. Infect. Immun. **77**:2030–2035.
35. **Reuveny S, et al.** 2001. Search for correlates of protective immunity conferred by anthrax vaccine. Infect. Immun. **69**:2888–2893.
36. **Rossi Paccani S, et al.** 2007. Anthrax toxins inhibit immune cell chemotaxis by perturbing chemokine receptor signalling. Cell. Microbiol. **9**:924–929.
37. **Subramanian GM, et al.** 2005. A phase 1 study of PAmAb, a fully human monoclonal antibody against Bacillus anthracis protective antigen, in healthy volunteers. Clin. Infect. Dis. **41**:12–20.
38. **Unkeless JC.** 1979. Characterization of a monoclonal antibody directed against mouse macrophage and lymphocyte Fc receptors. J. Exp. Med. **150**:580–596.
39. **Verma A, et al.** 2009. Analysis of the Fc gamma receptor-dependent component of neutralization measured by anthrax toxin neutralization assays. Clin. Vaccine Immunol. **16**:1405–1412.
40. **Vitale L, et al.** 2006. Prophylaxis and therapy of inhalational anthrax by a novel monoclonal antibody to protective antigen that mimics vaccine-induced immunity. Infect. Immun. **74**:5840–5847.
41. **Weiss S, et al.** 2006. Immunological correlates of protection against intranasal challenge of *Bacillus anthracis* spores conferred by a protective antigen-based vaccine in rabbits. Infect. Immun. **74**:394–398.
42. **Welkos S, Little S, Friedlander A, Fritz D, Fellows P.** 2001. The role of antibodies to Bacillus anthracis and anthrax toxin components in inhibiting the early stages of infection by anthrax spores. Microbiology **147**: 1677–1685.